Hearing Research 466 (2025) 109374

Contents lists available at ScienceDirect

Hearing Research

journal homepage: www.elsevier.com/locate/heares

Research Paper

Optimization of the Yacovino maneuver for superior canal BPPV using numerical simulations

Ismael Arán-Tapia [a,b,*], Guillermo Bastos [a,c], Alberto P. Muñuzuri [a,d]

[a] Group of Non-Linear Physics, University of Santiago de Compostela, Campus Sur, Spain
[b] Cross-Disciplinary Research Center in Environmental Technologies (CRETUS), University of Santiago de Compostela, Spain
[c] Telecommunications Engineering School, University of Vigo, Spain
[d] Galician Center for Mathematical Research and Technology (CITMAga), Santiago de Compostela, Spain

ARTICLE INFO

Keywords:
Benign paroxysmal positional vertigo
Yacovino maneuver
Computational fluid dynamics
Mathematical modeling

ABSTRACT

We evaluated the effectiveness of the original Yacovino maneuver (YM) for treating superior canal benign paroxysmal positional vertigo (SC-BPPV) using numerical simulations and proposed modifications to enhance its efficacy. A high-resolution three-dimensional micro-computed tomography (μCT) reconstruction of a human membranous labyrinth was used to simulate the BPPV condition. Endolymphatic fluid dynamics were modeled by solving the Navier–Stokes equations, and otoconia of varying sizes (3–30 μm) were introduced as Lagrangian particles. Their displacement was tracked using a superior canal-centric polar coordinate system. Two maneuver protocols were simulated: the original YM and a modified version with adjusted rotational angles and a 30-second resting interval per step. The original YM resulted in otoconia trapping in the ampulla and canal switching, limiting its effectiveness. In contrast, the modified YM—in which the patient lies face down with a 50° head flexion in the initial step, followed by optimized subsequent rotations—significantly improved otoconia migration toward the utricular macula. Longer resting times further enhanced the displacement of smaller particles without compromising maneuver safety. These findings suggest that the modified YM is a safe and effective alternative for SC-BPPV treatment. Tailoring rotation angles based on anatomical variability may improve outcomes, though clinical validation is still required.

1. Introduction

Benign Paroxysmal Positional Vertigo (BPPV) is a common vestibular disorder characterized by brief episodes of vertigo triggered by specific head movements. This condition occurs when otoconia, normally attached to the utricular macula, dislodge from their usual position and enter the semicircular canals. The posterior canal variant (PC-BPPV) has traditionally been reported to account for 60–90% of cases (Kim and Zee, 2014; von Brevern, 2013). However, more recent studies suggest that this prevalence may be overestimated, highlighting a more significant role for horizontal canal BPPV (HC-BPPV), found in 40–50% of cases (Bhandari et al., 2023a), and superior canal BPPV (SC-BPPV), with a reported occurrence ranging from 1% to 17% (Anagnostou et al., 2015). In addition, a history of head trauma may be associated with a higher incidence of SC-BPPV (Jackson et al., 2007).

Thus, SC-BPPV remains the rarest form of canalolithiasis, with a diagnosis that can be challenging and prone to misinterpretation as central neurological disorders due to similar nystagmus patterns (Bertholon et al., 2002; Bhandari et al., 2021a). Moreover, atypical variants of posterior canal BPPV can produce positional downbeat and torsional nystagmus resembling superior canal involvement (Garaycochea and Pérez-Fernández, 2024). These cases increase the risk of misdiagnosis and may contribute to the limited effectiveness of maneuvers targeting the superior canal.

Several canalith repositioning procedures (CRPs) have been proposed for treating SC-BPPV. Adapted versions of the Epley and Semont maneuvers, typically used for treating PC-BPPV, have shown success in treating SC-BPPV (Epley, 1992; Lopez-Escamez et al., 2006; Semont et al., 1988; Seok et al., 2008). Additionally, various other maneuvers have been explored for this purpose (D'Albora Rivas et al., 2020;

Abbreviations: BPPV, Benign paroxysmal positional vertigo; PC, posterior canal; HC, horizontal canal; SC, superior canal; CRP, canalith repositioning procedure; YM, Yacovino maneuver; μCT, micro-computed tomography; CFD, computational fluid dynamics.

* Corresponding author at: Group of Non-Linear Physics, University of Santiago de Compostela, Campus Sur, Spain.
E-mail address: ismaelaran.tapia@usc.es (I. Arán-Tapia).

https://doi.org/10.1016/j.heares.2025.109374
Received 18 June 2025; Received in revised form 20 July 2025; Accepted 21 July 2025
Available online 22 July 2025

Garaycochea et al., 2022; Rahko, 2002; Vannucchi et al., 2015).

All these CRPs require prior identification of the affected side. However, a maneuver proposed by Yacovino et al. has the advantage of not requiring precise identification of the affected SC (Yacovino et al., 2009). This maneuver involves rotating the patient forward and backward within the same plane of rotation. However, the simplicity of the Yacovino maneuver (YM) introduces limitations: the rotation plane does not align with the plane of the affected semicircular canal, since ideally, the SCs are positioned at a 45° angle relative to the sagittal plane used as the rotation plane. Moreover, it is essential to consider anatomical variations among individuals, including differences in semicircular canal angles (Della Santina et al., 2005; Johnson Chacko et al., 2018).

The design of the YM for a unique rotation plane that does not coincide with the affected canal plane, combined with human variability in semicircular canal orientation, could explain the significant disparity across clinical studies assessing the maneuver's effectiveness, with reported treatment success rates ranging from 36% to 100% (Califano et al., 2014; Marques et al., 2014; Yacovino et al., 2009; Yang et al., 2019). The limited number of studies and lack of large-scale clinical trials contribute to questions about the maneuver's validated efficacy.

Regarding previous studies employing numerical simulations on BPPV, these indicate the potential of using this non-invasive analytical tool to evaluate the displacement of otoconia during CRPs. Several mathematical models have elucidated the behavior of otoconia within the semicircular canals in the context of BPPV and have proposed modified maneuvers (Arán-Tapia et al., 2024; Boselli et al., 2014; House and Honrubia, 2003; Obrist and Hegemann, 2008; Rajguru et al., 2005, 2004; Squires et al., 2004). Most of these studies focused on other CRPs, but other computational approaches centered on treating SC-BPPV have indicated that the YM might not be efficient in its originally described form (Bhandari et al., 2021a, 2021b).

Under this hypothesis, we aim to study the effectiveness of the YM for a single subject by employing numerical simulations specific to their anatomy. We seek to assess whether modifying the degrees of rotation based on the anatomical properties of the subject can optimize the results while adhering to the original consideration of the YM, which treats both SCs simultaneously. In this context, we propose a modified YM that incorporates our observations from simulations, with the objective of supporting a more precise treatment.

2. Materials and methods

2.1. Geometric model

A three-dimensional medical image reconstruction of a right membranous labyrinth was used. It corresponds to a "post-mortem" human, obtained using high-quality micro-computed tomography (μCT) with a voxel size under 20 μm (David et al., 2016). Detailed information about the process of adapting the geometry to make it suitable as input for the mathematical analysis is found in our previous research (Arán-Tapia et al., 2023). A polyhedral mesh of 351,716 cells was selected for the fluid region, ensuring that the cell volume exceeds the otoconia volume to avoid numerical instabilities. A mesh independence analysis was performed to determine the optimal configuration for studying BPPV (see our previous study regarding the Epley maneuver for more details (Arán-Tapia et al., 2024)).

2.2. Mathematical model

The boundary of the geometric domain consists in rigid, no-slip wall, since elasticity is not relevant at the frequencies typically considered during CRPs (Breneman and Rabbitt, 2009; Iversen and Rabbitt, 2017; Rabbitt, 2019). The cupula walls were also assumed to be rigid because the fluid stream generated by cupula deflection is not strong enough to affect otoconia due to the difference in density: 2700 kg/m^3 of the otoconia (Squires et al., 2004) and 1000 kg/m^3 of the endolymph (David et al., 2016). A time-step of 1 ms was used.

A total of 10 otoconia were introduced in each simulation, ranging from 3 to 30 μm in increments of 3 μm, which reflects the size observed in humans (Jang et al., 2006). Due to the small ratio particle-volume-to-fluid-volume (Boselli et al., 2014), collisions between particles were not simulated to reduce computational costs.

The flow of the endolymphatic fluid around otoconia was modeled as laminar with a dynamic viscosity of $8.15{\cdot}10^{-4}$ Pa·s (David et al., 2016), given the typically low Reynolds number in endolymph ($Re \approx 10^{-3}$–10^{-2}) (Brody et al., 1996; Hain et al., 2005). The Froude number shows that inertial and gravity forces are equally important during the rotations. Then, the solution for the endolymphatic flow is obtained by solving the Navier–Stokes equations, incorporating the inertial terms resulting from the rotation of the patient's body. The displacement of the otoconia is determined by the same forces present in the Navier-Stokes equations, together with the buoyancy and gravitational forces. A more detailed explanation of the computational fluid dynamics (CFD) mathematical model and its limitations can be found in our previous study (Arán-Tapia et al., 2024).

2.3. Coordinate systems for rotation

The rotations in our model were centered at either the head or the waist center. The distance between the head and waist origins is typically 75 cm (Roser et al., 2013). The orientations of both coordinate systems remain consistently aligned regardless of the step considered, which means that all rotations were applied using the same reference axes. This ensures that rotational directions and angles are interpreted uniformly throughout the simulation, independent of the rotation origin.

A third coordinate system, referred to as the superior coordinate system, was introduced to report the position of each otoconia relative to the centroid of the canal. It was employed to describe numerical simulation results based on the angular position of the otoconia using polar coordinates. To quantify the advance of the otoconia, the angular polar coordinate was set to zero at the beginning of each step.

2.4. Definition of the original and modified Yacovino maneuvers

The original YM was simulated following the procedure described originally (Yacovino et al., 2009). In contrast, the modified YM incorporates several modifications based on observations from the numerical results of the original maneuver. The prescribed angles for both maneuvers are listed in Table 1 and Table 2, respectively. Positive rotations indicate counterclockwise movement, while negative rotations indicate clockwise movement.

The modified YM is presented in Fig. 1. First, the patient begins in a standing position next to the bed. Instead of being asked to lie face up, the patient is instructed to lie face down. This can be considered as a rotation of the body by +90° relative to the waist in step 1A (Fig. 1a). Subsequently, in step 1B (Fig. 1b), the head is flexed through an angle ranging from +45° to +60° to determine the optimal position.

Next, in step 2A, the patient rotates 180° around the X-axis at the waist (Fig. 1c), transitioning from a prone to a supine position while keeping the head orientation fixed relative to the body. Both rotations—toward the healthy and the affected side—were considered.

Table 1
Steps and substeps of the original version of YM.

Step	Plane of rotation	Origin	Rotation (°)
1A	(0, 1, 0)	Waist	−90
1B	(0, 1, 0)	Head	−30
2	(0, 1, 0)	Head	+75
3A	(0, 1, 0)	Waist	+90
3B	(0, 1, 0)	Head	−45

Table 2
Steps and substeps studied for the modified version of the YM, along with the optimal rotation degrees derived from numerical results.

Step	Plane of rotation	Origin	Simulated rotations (°)	Optimal rotation (°)
1A	(0, 1, 0)	Waist	+90	+90
1B	(0, 1, 0)	Head	+45, +50, +55, +60	+50
2A	(1, 0, 0)	Waist	+180, −180	±180
2B	(0, 1, 0)	Head	+80	+80
3	(0, 1, 0)	Head	−30, −35, −40, −45, −50, −55, −60	−45
4	(0, 1, 0)	Waist	−135, −140, −145, −150	−150

Importantly, after this 180° rotation, the interpretation of positive and negative Y-axis rotations becomes inverted, since the same global axis orientation is maintained throughout the simulation. Consequently, in step 2B (Fig. 1d), a positive 80° Y-rotation corresponds to a head extension, positioning the head below the horizontal plane. Different excursion angles were not studied, as the aim is to reposition the head according to the original definition of the YM: the head should hang 30° below the horizontal plane.

During step 3, the head is flexed as defined in the original maneuver, but a different range of rotations from −30° to −60° is examined to identify the optimal position for the otoconia (Fig. 1e).

Finally, in step 4, the patient's body is rotated through an angle ranging between −135° and −150°, while maintaining the head orientation defined in the previous step (Fig. 1f). After completing this step and a resting period, the patient returns to a sitting position or stands up to finish the maneuver.

The modifications were based on the initial aim of the original maneuver; therefore, the rotations are performed in the sagittal plane (except for step 2A, which does not involve significant otoconia displacement). Each rotation in the simulation takes 3 s, and a resting period of 30 s is applied at the end of each complete step. The optimal degree of rotation is selected based on the maximum displacement of the otoconia during this 30-second period. At the beginning of a new step, all otoconia are positioned as they would be after an infinite period of time.

3. Results

After analyzing the numerical results, we identified three potential failures in the definition of the original YM, as illustrated in Fig. 2. First, we found that the otoconia became trapped in the ampulla during step 1B (Fig. 2a). To allow for further analysis of the subsequent maneuver steps, we artificially repositioned the otoconia far enough from the ampulla. Next, during step 2 (Fig. 2b), we observed otoconia entering the PC. Again, to overcome this limitation, we placed the otoconia at the exit of the SC to proceed with the maneuver. Finally, the maneuver fails in the last step because ending with the head in a straight position causes the otoconia to move into the posterior short arm, ultimately getting trapped in the posterior ampulla instead of reaching the utricular macula (Fig. 2c).

Fig. 1 provides a visual representation of the final configuration of the modified YM, illustrating the head and left membranous labyrinth orientations selected for each step. These specific planes of rotation were chosen based on the range of angles evaluated in Table 2. Fig. 3 graphically summarizes the numerical results from testing these different rotations, showing the total displacement of otoconia after 30 s of resting time as a function of particle size and rotation angle. This analysis supports the selection of the optimal angles implemented in the modified maneuver (see Supplementary Video 1).

The results for step 1B are summarized in Fig. 3a, indicating that a rotation angle greater than 50° significantly increases the displacement of the otoconia, allowing them to exit the superior ampulla (Fig. 1a and 1b).

In the following step, step 2A, the patient's position transitions from prone to supine by rotating 180° around the X-axis at the waist (Fig. 1c). The direction of this rotation—whether toward the affected or healthy side—did not result in significant differences in otoconia displacement. According to the numerical simulations, the angular difference in the final position of the particles was 4.0° for the heaviest and 0.2° for the lightest otoconia. Then, in step 2B, the head is extended by 80°, resulting in a final position where it hangs approximately 30° below the horizontal plane (Fig. 1d), mimicking the position achieved at the end of step 1 in the original YM.

The results from step 3, where the patient's head is rotated nose-down (Fig. 1e), are summarized in Fig. 3b. These results indicate that a rotation angle lower than 50° is crucial to prevent the otoconia from entering the PC, while a very small rotation would lead to minimal displacement of otoconia during this step.

Finally, in step 4, the patient is raised by rotating their torso 150° at the waist, finishing in a final position of approximately 75° nose-down. This position was found to be optimal (Fig. 3c), as it enhances the displacement of otoconia while ensuring that they remain in the utricular macula (Fig. 1f).

4. Discussion

After analyzing the numerical simulations, we encountered certain limitations that may contradict the success of the original YM. For this reason, we suggested adaptations to the standard maneuver to facilitate the advancement of otoconia inside the SC and allow them to reach the utricular macula. All these adaptations are presented in Fig. 1 and Table 2.

Otoconia may become trapped in the superior ampulla during the first step of the original YM (Fig. 2a), which could render the remainder of the maneuver ineffective since the otoconia are not displaced along the SC as desired. Other studies employing real-time animations based on Unity 3D software have not described this effect during the study of the YM (Bhandari et al., 2021a, 2021b). However, another study using Unity 3D observed a similar situation when exploring the supine hanging head position—a diagnostic maneuver that employs a rotation similar to the first step of the original YM (Li and Yang, 2023). For that reason, this appears to be more of a limitation of the anatomical model than due to the software employed. An inaccurate 3D model of the membranous labyrinth leads to erroneous results, as likely occurs if the superior ampulla morphology is omitted.

To overcome this limitation, we concluded that an extra step is required to expel the otoconia from the ampulla during step 1A (Fig. 1a), when the patient lies face down on the bed, thus allowing the advancement of otoconia during the resting period after step 1B (Fig. 1b). The application of a head flexion angle larger than 50° in this last substep appears sufficient for the otoconia to exit the ampulla and for the heaviest particles to reach the lowest point of the canal in the patient's oriented position. If possible, a 60° angle would allow for a larger displacement of smaller otoconia (Fig. 3a), although this may be challenging due to neck restrictions (Martellucci et al., 2019).

After this step, we perform a body rotation in step 2A (Fig. 1c). The final position of the particles varies little depending on the side to which the rotation is performed. The likely reason is that, during this specific step, otoconia displacement occurs mainly due to inertial forces generated during the rotation itself, rather than gravity, since no subsequent resting period was included (Arán-Tapia et al., 2024). As a result, overall particle movement remains confined to the same section of the canal, because the inertial forces generated by X-axis rotation in this configuration do not favor advancement along the canal. To conclude this step, the patient is positioned similarly to the original step 1 of the YM, but now the otoconia are able to advance through the SC (Fig. 1d). In a real treatment scenario, the doctor could execute both substeps simultaneously, which should improve the efficacy of the procedure.

Another limitation observed during the original YM is the possible

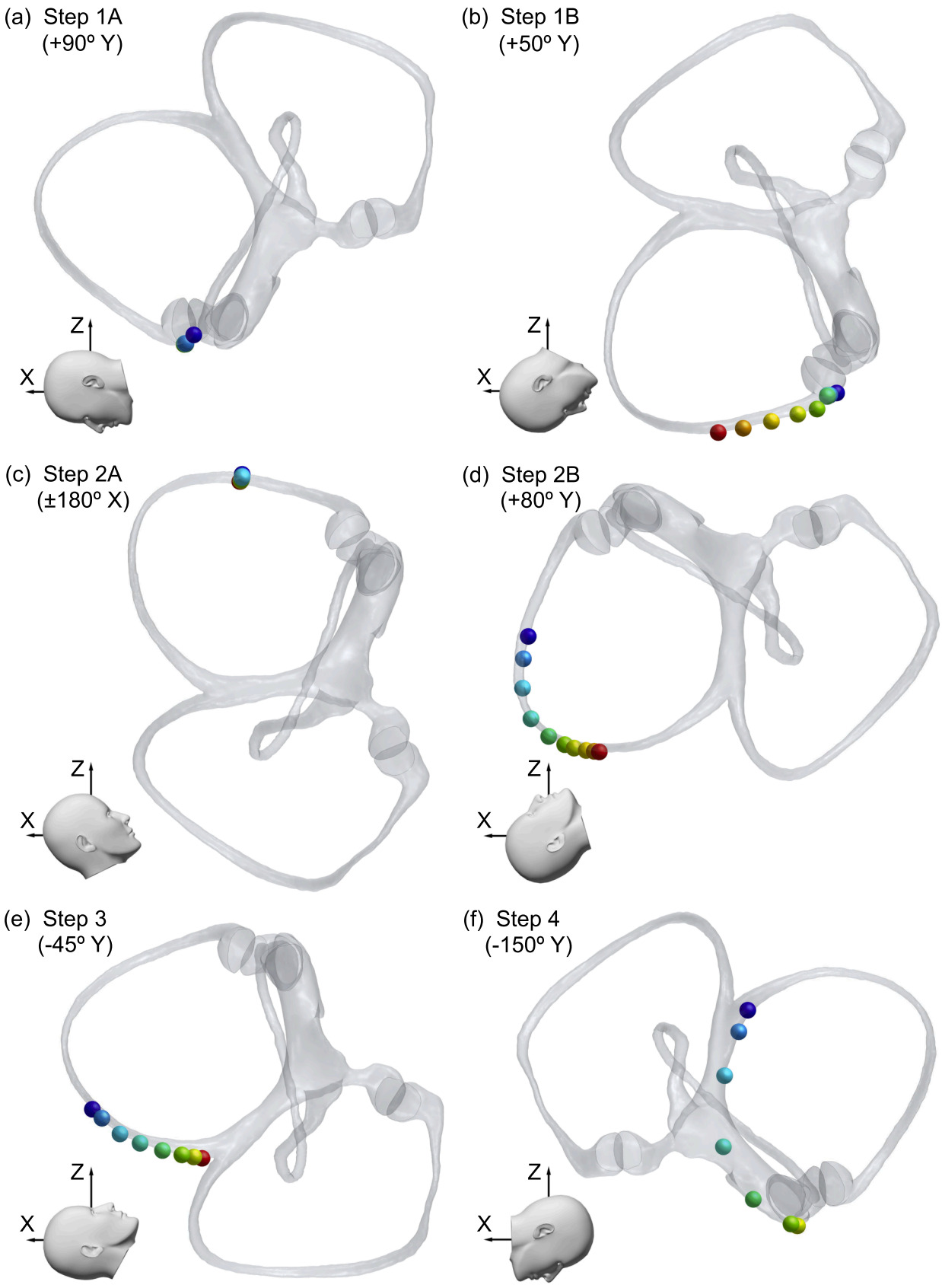

Fig. 1. Head and left membranous labyrinth orientations during each step of the modified YM. Optimal rotation angles and axes, derived from numerical results (see Table 2), are indicated for each step. Otoconia are depicted as enlarged spherical particles, with a color code ranging from the larger size (30 μm, red) to the smaller size (3 μm, blue) for (a) step 1A, (b) step 1B, (c) step 2A, (d) step 2B, (e) step 3, and (f) step 4.

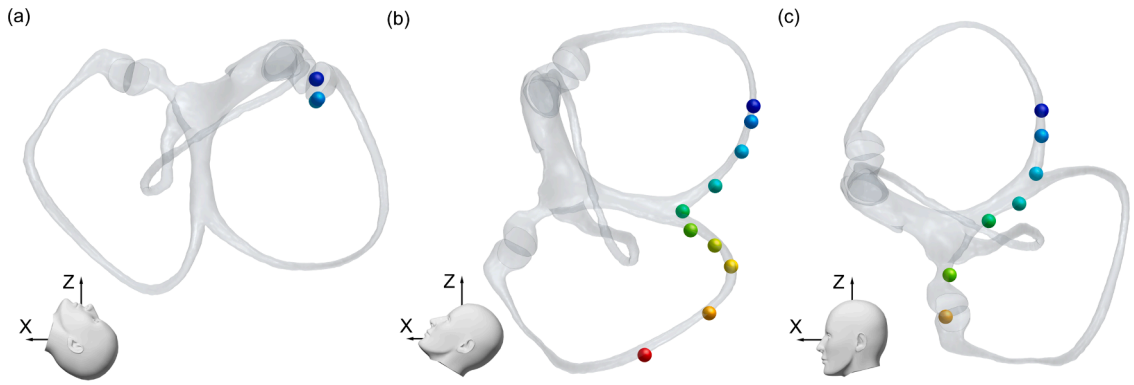

Fig. 2. Representation of the three potential failures in the definition of the original YM. Following the same criteria as in Fig. 1, this figure illustrates the original orientations in (a) step 1B, (b) step 2, and (c) step 3B.

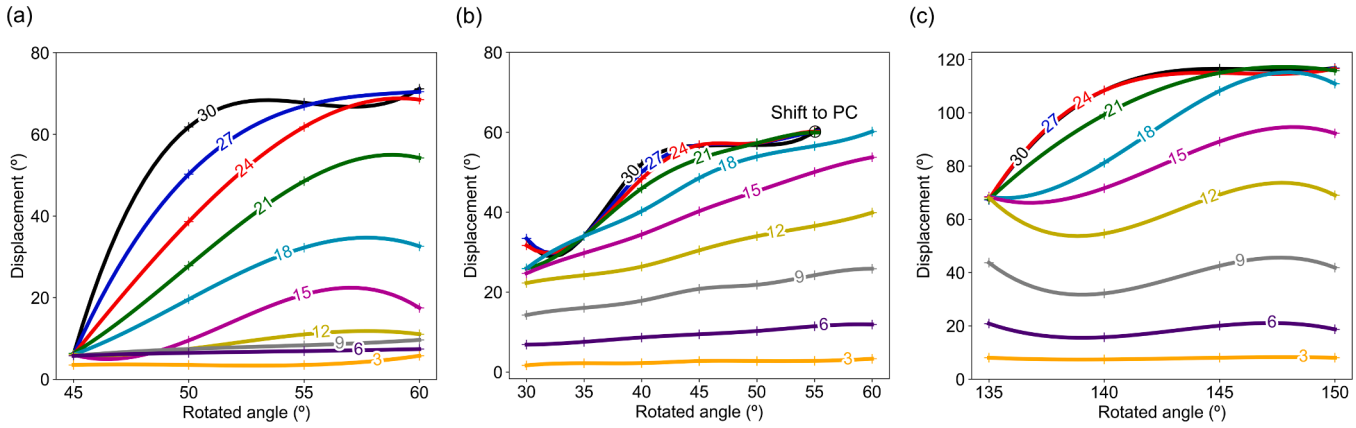

Fig. 3. Otoconia displacement analysis for the rotation angles studied in the modified YM. Data are interpolated to show the total displacement for each otoconia size after a 30 s resting period in (a) step 1B, (b) step 3, and (c) step 4.

canal switch from the SC to the PC during step 2 (Fig. 2b). This type of canal switch has been previously documented for CRPs (Arán-Tapia et al., 2024; Park et al., 2013; Wu et al., 2022), including the YM (Bhandari et al., 2021a). In that study, they recommended a modification that involves seating the patient immediately after the first step. However, given the resting time employed and the limitations described in the previous step, smaller otoconia may still be present near the exit of the ampulla. As a result, performing this step could cause them to return to the superior ampulla, allowing only the larger otoconia to be successfully treated.

What we propose is a modification with a smaller rotation than the original definition of the YM—approximately 45° of head flexion to keep the head slightly above the horizontal plane during the step 3 (Fig. 1e). This adjustment allows the otoconia to continue their path away from the ampulla while minimizing the risk of otoconia moving from the SC to the PC (Fig. 3b). It is important to note that the anatomical variability of the common crux and the semicircular canals may significantly affect the optimal angle required for the patient (Della Santina et al., 2005; Johnson Chacko et al., 2018). For that reason, positioning the patient on a horizontal plane may be a safer treatment option, in anticipation of a possible lack of efficacy in otoconia displacement.

After that, the original YM includes a final step that consists of returning the patient to a sitting position. If this step is performed, we observed that otoconia fall into the posterior ampulla from the short arm (Fig. 2c), similar to what occurs during the Epley maneuver in the same vestibular anatomy (Arán-Tapia et al., 2024). For that reason, a body or head flexion resulting in a 75° nose-down position would cause the otoconia to reach the utricular macula (Fig. 1f), thereby facilitating re-fixation (Otsuka et al., 2010). In the study we performed, this consisted of a body rotation of 150° relative to the previous position (Fig. 3c). However, it is possible to combine body and head movements to facilitate achieving this final position for the patient.

Another important aspect of the YM, similar to any other CRP, is the resting time employed. Optimization can be approached from two perspectives: adjusting the maneuver based on the labyrinth orientation (Fig. 1) or adapting the resting time to accommodate the otoconia size. We have observed that the original maneuver does not seem successful, and this limitation cannot be re-solved by simply increasing the resting time (Fig. 2); however, our modified YM remains safe regardless of the resting time used. Longer resting periods beyond 30 s would simply allow smaller otoconia sufficient time to achieve their final position for each step, thereby potentially increasing success and reducing residual dizziness or nystagmus after treatment (Özgirgin et al., 2024). It is also recommended to employ a rotary chair, which can enhance accuracy in the rotation angles compared to manual application (Abdulovski and Klokker, 2021; Bhandari et al., 2023b; Moroz et al., 2021).

This study has several limitations inherent to the use of a computational model. First, simulations were performed using a single human anatomical reconstruction, which does not account for inter-individual variability in canal geometry or orientation. Second, although a range of otoconia sizes was considered, the model assumes an idealized, low number of free-floating spherical particles, without accounting for possible clumping, collisions, or adhesion between particles or to the elastic canal walls. These effects could alter otoconia trajectories and potentially impact the optimal definition of the maneuver. Simulating this more complex scenario is planned for future work; however, incorporating such features significantly increases computational cost and simulation time. While the present results offer valuable

biomechanical insights, clinical validation is necessary to determine the generalizability of the maneuver and to assess whether a personalized approach is needed, given the complex and patient-specific variability in BPPV anatomy, otoconia distribution, and physical properties.

5. Conclusions

Through detailed CFD simulations based on a μCT of a specific human membranous labyrinth, we observed that the original YM is prone to trap the otoconia in the superior ampulla and canal switching from the SC to the PC. Consequently, we propose a modification of the YM designed to guide the otoconia through the SC in a safer and more controlled manner. This approach yields better outcomes compared to the original YM in terms of otoconia displacement. In this context, we suggest that our modified maneuver could be useful for a broader range of subjects, although achieving optimal results may require a personalized approach based on individual anatomical properties. Finally, a clinical study should be conducted to test the efficacy of the proposed modifications. This evaluation has already been discussed with clinical collaborators and is considered a relevant next step to validate the numerical findings in real patients.

Ethics approval and consent to participate

This study utilized a human micro-computed tomography from an open-source database (http://www.earbank.org/ariadne.php). Since no direct clinical study of patients was conducted, ethics approval or consent to participate was not required.

Consent for publication

Not applicable.

Funding

This research is supported by the Spanish Ministerio de Economía y Competitividad and the European Regional Development Fund, through research grant PID2022–138322OB-100, funded by MCIN/AEI/10.13039/501100011033 and by "ERDF A Way of Making Europe." It is also supported by Xunta de Galicia under research grant no. 2021-PG036, and the Instituto de Salud Carlos III (ISCIII) under grant number PI23/00248.

CRediT authorship contribution statement

Ismael Arán-Tapia: Writing – original draft, Visualization, Validation, Supervision, Software, Methodology, Investigation, Formal analysis, Conceptualization. **Guillermo Bastos:** Writing – original draft, Visualization, Validation, Software, Investigation, Formal analysis, Data curation. **Alberto P. Muñuzuri:** Writing – review & editing, Supervision, Resources, Project administration, Funding acquisition, Conceptualization.

Declaration of competing interest

All authors declare no competing interest related to this article.

Acknowledgement

The simulations were run at the Supercomputer Center of Galicia (CESGA), and we acknowledge their support. We also acknowledge the use of OpenAI's ChatGPT (GPT-4o) for assisting in the correction of English language and enhancing the clarity of the manuscript.

Supplementary materials

Supplementary material associated with this article can be found, in the online version, at doi:10.1016/j.heares.2025.109374.

Data availability

All data generated or analyzed during the present study has been incorporated into this published article and its supplementary information files. The original datasets used and analyzed during the current study are available from the corresponding author upon reasonable request.

References

Abdulovski, S., Klokker, M., 2021. Repositioning chairs in the diagnosis and treatment of benign paroxysmal positional vertigo–a systematic review. J. Int. Adv. Otol. 17, 353–360. https://doi.org/10.5152/iao.2021.9434.

Anagnostou, E., Kouzi, I., Spengos, K., 2015. Diagnosis and treatment of anterior-canal benign paroxysmal positional vertigo: a systematic review. J. Clin. Neurol. 11, 262–267. https://doi.org/10.3988/jcn.2015.11.3.262.

Arán-Tapia, I., Soto-Varela, A., Pérez-Muñuzuri, V., Santos-Pérez, S., Arán, I., Muñuzuri, A., 2024. Numerical simulations of the epley maneuver with clinical implications. Ear Hear. 45, 1033–1044. https://doi.org/10.1097/AUD.0000000000001493.

Arán-Tapia, I., Soto-Varela, A., Pérez-Muñuzuri, V., Santos-Pérez, S., Arán, I., Muñuzuri, A.P., 2023. Numerical simulations to determine the stimulation of the crista ampullaris during the Head impulse test. Comput. Biol. Med. 163, 107225. https://doi.org/10.1016/j.compbiomed.2023.107225.

Bertholon, P., Bronstein, A.M., Davies, R.A., Rudge, P., Thilo, K.V., 2002. Positional down beating nystagmus in 50 patients: cerebellar disorders and possible anterior semicircular canalithiasis. J. Neurol. Neurosurg. Psychiatry 72, 366–372. https://doi.org/10.1136/jnnp.72.3.366.

Bhandari, A., Bhandari, R., Kingma, H., Strupp, M., 2021a. Diagnostic and therapeutic maneuvers for anterior canal BPPV canalithiasis: three-dimensional simulations. Front. Neurol. 12, 740599. https://doi.org/10.3389/fneur.2021.740599.

Bhandari, A., Kingma, H., Bhandari, R., 2021b. BPPV simulation: a powerful tool to understand and optimize the diagnostics and treatment of all possible variants of BPPV. Front. Neurol. 12, 632286. https://doi.org/10.3389/fneur.2021.632286.

Bhandari, R., Bhandari, A., Hsieh, Y., Edlow, J., Omron, R., 2023a. Prevalence of horizontal canal variant in 3975 patients with benign paroxysmal positional Vertigo: a cross-sectional study. Neurol. Clin. Pract. 13, e200191. https://doi.org/10.1212/CPJ.0000000000200191.

Bhandari, R., Bhandari, A., Kingma, H., van de Berg, R., 2023b. Large variability of head angulation during the epley maneuver: use of a head-mounted guidance system with visual feedback to improve outcomes. J. Int. Adv. Otol. 19, 234–241. https://doi.org/10.5152/iao.2023.22969.

Boselli, F., Kleiser, L., Bockisch, C.J., Hegemann, S.C.A., Obrist, D., 2014. Quantitative analysis of benign paroxysmal positional vertigo fatigue under canalithiasis conditions. J. Biomech. 47, 1853–1860. https://doi.org/10.1016/j.jbiomech.2014.03.019.

Breneman, K.D., Rabbitt, R.D., 2009. Piezo- and flexoelectric membrane materials underlie fast biological motors in the ear. Mater. Res. Soc. Symp. Proc. 1186E. https://doi.org/10.1557/PROC-1186-JJ06-04, 1186-JJ06-04.

Brody, J.P., Yager, P., Goldstein, R.E., Austin, R.H., 1996. Biotechnology at low Reynolds numbers. Biophys. J. 71, 3430–3441. https://doi.org/10.1016/S0006-3495(96)79538-3.

Califano, L., Salafia, F., Mazzone, S., Melillo, M.G., Califano, M., 2014. Anterior canal BPPV and apogeotropic posterior canal BPPV: two rare forms of vertical canalolithiasis. Acta Otorhinolaryngol. Ital. 34, 189–197.

D'Albora Rivas, R., Teixido, M., Casserly, R.M., Mónaco, M.J., 2020. Short CRP for anterior canalithiasis: a new maneuver based on simulation with a biomechanical model. Front. Neurol. 11, 857. https://doi.org/10.3389/fneur.2020.00857.

David, R., Stoessel, A., Berthoz, A., Spoor, F., Bennequin, D., 2016. Assessing morphology and function of the semicircular duct system: introducing new *in-situ* visualization and software toolbox. Sci. Rep. 6, 32772. https://doi.org/10.1038/srep32772.

Della Santina, C.C., Potyagaylo, V., Migliaccio, A.A., Minor, L.B., Carey, J.P., 2005. Orientation of human semicircular canals measured by three-dimensional multiplanar CT reconstruction. J. Assoc. Res. Otolaryngol. 6, 191–206. https://doi.org/10.1007/s10162-005-0003-x.

Epley, J.M., 1992. The canalith repositioning procedure: for treatment of benign paroxysmal positional vertigo. Otolaryngol. Head Neck Surg. 107, 399–404. https://doi.org/10.1177/019459989210700310.

Garaycochea, O., Pérez-Fernández, N., 2024. Variants of posterior semicircular canal involvement in benign paroxysmal positional vertigo. Acta Otorrinolaringol. (Engl. Ed.) 75, 324–334. https://doi.org/10.1016/j.otoeng.2024.01.013.

Garaycochea, O., Pérez-Fernández, N., Manrique-Huarte, R., 2022. A novel maneuver for diagnosis and treatment of torsional-vertical down beating positioning nystagmus: anterior canal and apogeotropic posterior canal BPPV. Braz. J. Otorhinolaryngol. 88, 708–716. https://doi.org/10.1016/j.bjorl.2020.09.009.

Hain, T.C., Squires, T.M., Stone, H.A., 2005. Clinical implications of a mathematical model of benign paroxysmal positional vertigo. Ann. NY Acad. Sci. 1039, 384–394. https://doi.org/10.1196/annals.1325.036.

House, M.G., Honrubia, V., 2003. Theoretical models for the mechanisms of benign paroxysmal positional vertigo. Audiol. Neurootol. 8, 91–99. https://doi.org/10.1159/000068998.

Iversen, M.M., Rabbitt, R.D., 2017. Wave mechanics of the vestibular semicircular canals. Biophys. J. 113, 1133–1149. https://doi.org/10.1016/j.bpj.2017.08.001.

Jackson, L., Morgan, B., Fletcher, J., Krueger, W., 2007. Anterior canal benign paroxysmal positional vertigo: an underappreciated entity. Otol. Neurotol. 28, 218–222. https://doi.org/10.1097/01.mao.0000247825.90774.6b.

Jang, Y.S., Hwang, C.H., Shin, J.Y., Bae, W.Y., Kim, L.S., 2006. Age-related changes on the morphology of the otoconia. Laryngoscope 116, 996–1001. https://doi.org/10.1097/01.mlg.0000217238.84401.03.

Johnson Chacko, L., Schmidbauer, D.T., Handschuh, S., Reka, A., Fritscher, K.D., Raudaschl, P., Saba, R., Handler, M., Schier, P.P., Baumgarten, D., Fischer, N., Pechriggl, E.J., Brenner, E., Hoermann, R., Glueckert, R., Schrott-Fischer, A., 2018. Analysis of vestibular labyrinthine geometry and variation in the Human temporal bone. Front. Neurosci. 12, 107. https://doi.org/10.3389/fnins.2018.00107.

Kim, J.S., Zee, D.S., 2014. Clinical practice. Benign paroxysmal positional vertigo. N. Engl. J. Med. 370, 1138–1147. https://doi.org/10.1056/NEJMcp1309481.

Li, Y., Yang, X., 2023. Design and analysis of HSC-BPPV diagnostic maneuver based on virtual simulation. Front. Neurol. 14, 1132343. https://doi.org/10.3389/fneur.2023.1132343.

Lopez-Escamez, J.A., Molina, M.I., Gamiz, M.J., 2006. Anterior semicircular canal benign paroxysmal positional vertigo and positional downbeating nystagmus. Am. J. Otolaryngol. 27, 173–178. https://doi.org/10.1016/j.amjoto.2005.09.010.

Marques, P., Castillo, R., Santos, M., Perez-Fernandez, N., 2014. Repositioning nystagmus: prognostic usefulness? Acta Otolaryngol. 134, 491–496. https://doi.org/10.3109/00016489.2013.872291.

Martellucci, S., Attanasio, G., Ralli, M., Marcelli, V., de Vincentiis, M., Greco, A., Gallo, A., 2019. Does cervical range of motion affect the outcomes of canalith repositioning procedures for posterior canal benign positional paroxysmal vertigo? Am. J. Otolaryngol. 40, 494–498. https://doi.org/10.1016/j.amjoto.2019.04.003.

Moroz, M., Choy, M., Lee, C.W., Hadfield, H., Lasenby, J., Stone, T., Bance, M., 2021. Evaluating the epley canalolith repositioning procedure with and without a visual assistive device. Otol. Neurotol. 42, 765–773. https://doi.org/10.1097/MAO.0000000000003017.

Obrist, D., Hegemann, S., 2008. Fluid-particle dynamics in canalithiasis. J. R. Soc. Interface 5, 1215–1229. https://doi.org/10.1098/rsif.2008.0047.

Otsuka, K., Suzuki, M., Shimizu, S., Konomi, U., Inagaki, T., Iimura, Y., Hayashi, M., Ogawa, Y., 2010. Model experiments of otoconia stability after canalith repositioning procedure of BPPV. Acta Otolaryngol. 130, 804–809. https://doi.org/10.3109/00016480903456318.

Özgirgin, O.N., Kingma, H., Manzari, L., Lacour, M., 2024. Residual dizziness after BPPV management: exploring pathophysiology and treatment beyond canalith repositioning maneuvers. Front. Neurol. 15, 1382196. https://doi.org/10.3389/fneur.2024.1382196.

Park, S., Kim, B., Kim, S., Chu, H., Song, M., Kim, M., 2013. Canal conversion between anterior and posterior semicircular canal in benign paroxysmal positional vertigo. Otol. Neurotol. 34, 1725–1728. https://doi.org/10.1097/MAO.0b013e318294227a.

Rabbitt, R.D., 2019. Semicircular canal biomechanics in health and disease. J. Neurophysiol. 121, 732–755. https://doi.org/10.1152/jn.00708.2018.

Rahko, T., 2002. The test and treatment methods of benign paroxysmal positional vertigo and an addition to the management of vertigo due to the superior vestibular canal (BPPV-SC). Clin. Otolaryngol. Allied Sci. 27, 392–395. https://doi.org/10.1046/j.1365-2273.2002.00602.x.

Rajguru, S.M., Ifediba, M.A., Rabbitt, R.D., 2005. Biomechanics of horizontal canal benign paroxysmal positional vertigo. J. Vestib. Res. 15, 203–214.

Rajguru, S.M., Ifediba, M.A., Rabbitt, R.D., 2004. Three-dimensional biomechanical model of benign paroxysmal positional vertigo. Ann. Biomed. Eng. 32, 831–846. https://doi.org/10.1023/b:abme.0000030259.41143.30.

Roser, M., Appel, C., Ritchie, H., 2013. Human Height. Our World in Data.

Semont, A., Freyss, G., Vitte, E., 1988. Curing the BPPV with a liberatory maneuver. Adv. Otorhinolaryngol. 42, 290–293. https://doi.org/10.1159/000416126.

Seok, J.I., Lee, H.M., Yoo, J.H., Lee, D.K., 2008. Residual dizziness after successful repositioning treatment in patients with benign paroxysmal positional Vertigo. J. Clin. Neurol. 4, 107–110. https://doi.org/10.3988/jcn.2008.4.3.107.

Squires, T.M., Weidman, M.S., Hain, T.C., Stone, H.A., 2004. A mathematical model for top-shelf vertigo: the role of sedimenting otoconia in BPPV. J. Biomech. 37, 1137–1146. https://doi.org/10.1016/j.jbiomech.2003.12.014.

Vannucchi, P., Pecci, R., Giannoni, B., Di Giustino, F., Santimone, R., Mengucci, A., 2015. Apogeotropic posterior semicircular canal benign paroxysmal positional vertigo: some clinical and therapeutic considerations. Audiol. Res. 5, 130. https://doi.org/10.4081/audiores.2015.130.

von Brevern, M., 2013. Benign paroxysmal positional vertigo. Semin. Neurol. 33, 204–211. https://doi.org/10.1055/s-0033-1354590.

Wu, S., Li, J., Zhou, M., Yang, X., 2022. Simulation study of canal switching in BPPV. Front. Neurol. 13, 944703. https://doi.org/10.3389/fneur.2022.944703.

Yacovino, D.A., Hain, T.C., Gualtieri, F., 2009. New therapeutic maneuver for anterior canal benign paroxysmal positional vertigo. J. Neurol. 256, 1851–1855. https://doi.org/10.1007/s00415-009-5208-1.

Yang, X., Ling, X., Shen, B., Hong, Y., Li, K., Si, L., Kim, J.S., 2019. Diagnosis strategy and Yacovino maneuver for anterior canal-benign paroxysmal positional vertigo. J. Neurol. 266, 1674–1684. https://doi.org/10.1007/s00415-019-09312-1.